

Ultrathin, ultrasmooth, and low-loss silver films via wetting and annealing

W. Chen,¹ K. P. Chen,¹ M. D. Thoreson,² A. V. Kildishev,¹ and V. M. Shalaev^{1,a)}

¹Birck Nanotechnology Center and School of Electrical and Computer Engineering, Purdue University, West Lafayette, 47907 Indiana, USA

²Erlangen Graduate School in Advanced Optical Technologies (SAOT), Universität Erlangen-Nürnberg, 91052 Erlangen, Germany

(Received 25 July 2010; accepted 20 October 2010; published online 23 November 2010)

We have demonstrated that a thermal annealing treatment can reduce the optical losses in ultrathin, ultrasmooth, silver films deposited on a Ge wetting layer to values as low as the bulk material value and at the same time maintain an ultrasmooth surface. The annealing effect is sensitive to the annealing temperature and time, both of which should be carefully controlled. This annealing treatment is also effective for Ag–SiO₂ multilayer composite films. © 2010 American Institute of Physics. [doi:10.1063/1.3514257]

Silver (Ag) is the most-often used metal^{1,2} in recent optical metamaterial applications such as negative-index materials (NIMs),^{3,4} near-field superlenses⁶ and far-field hyperlenses.⁶ The properties of a silver film (SF), including the roughness, the minimum uniform thickness, and the optical loss, are vital to achieving good performance from metamaterials and other Ag-based plasmonic devices. A significant hurdle in superlens and hyperlens fabrication is that the required SFs or Ag-dielectric composite films often exhibit high surface roughness, which limits their overall imaging capabilities. In addition, the desired minimum thickness is often below the typical achievable minimum thickness (~20 nm) for continuous SFs fabricated on dielectrics such as silica (SiO₂).⁷ Recent reports have demonstrated a method to achieve an ultrathin and ultrasmooth SF using a very thin germanium (Ge) layer as a wetting material.^{7,8} However, such ultrathin, ultrasmooth SFs show five to ten times higher loss than that of bulk Ag due to the quantum size effect, which severely limits the applications of such films in realistic devices.

In this letter, we demonstrate a rapid thermal annealing treatment to reduce the ultrathin SF losses significantly by enlarging the internal grain sizes, bringing the loss close to that of bulk silver. A group of Ag/Ge/SiO₂/glass samples were fabricated using an electron-beam evaporation system (CHA Industries Model 600); different layers were deposited sequentially on the initial substrates without breaking the chamber vacuum. First, a 10 nm SiO₂ was deposited on the glass substrate to form the initial SiO₂ substrate surface. Next, a 1 nm Ge layer was deposited as a wetting layer. Finally, an Ag layer (10–20 nm) was deposited on the Ge/SiO₂/glass substrate. The evaporation chamber base pressure was about 1×10^{-6} Torr, and the evaporation rates were 0.05 nm/s for Ag and Ge and 0.1 nm/s for SiO₂. After the samples were fabricated and characterized, the annealing treatments were accomplished using a temperature-controllable electrical hotplate.

The far-field spectral responses (transmittance T and reflectance R) of the Ag/Ge/SiO₂/glass and 1 nm Ge/10 nm SiO₂/glass samples were measured every 5 nm in a wavelength range of 400–1700 nm with a spectrophotometer

(PerkinElmer Lambda 950) and an integrating sphere accessory. The absorptance (A) values were obtained as $A = 1 - T - R$. In order to better understand our experimental results, the Ge/SiO₂/glass and Ag/Ge/SiO₂/glass multilayer structures were modeled and analyzed using an analytical T-matrix method.^{9,10}

First, the far-field spectra of the 1 nm Ge/10 nm SiO₂/glass structure, which is used as a substrate for the SFs, were measured and analyzed through the T-matrix method. Figure 1(a) shows that the retrieved loss (ϵ'') from the measured spectra of a 1 nm Ge film is much lower than the bulk Ge value, and the loss peak around 550 nm disappears for the thin film. Moreover, the loss of the 1 nm Ge was further reduced by annealing at 320 °C for 3 min. From these considerations on the 1 nm Ge film (low loss and extremely thin layer thickness), we conclude that the loss contributed from the 1 nm Ge film to the total system loss is negligible.

The Ag dielectric constant can be described using the Drude–Lorentz model^{1,11} with a sum of Lorentz oscillators as shown in Eq. (1), where we have used five oscillators.

$$\epsilon = \epsilon_1 - \frac{\omega_p^2}{\omega^2 + i\gamma_p\omega} + \sum_{m=1}^5 \frac{f_m\omega_m^2}{\omega_m^2 - \omega^2 - i\gamma_m\omega}. \quad (1)$$

Here in the Drude term, $\epsilon_1 = 2.485$ is the static (infinite-frequency) dielectric constant, $\omega_p = 9.1821$ eV is the plasma frequency, and γ_p is the damping rate for the Drude term, which is the determining factor for the loss in the metal at optical frequencies. We used the values from Ref. 11 for the Lorentz terms. The Lorentz terms mainly contribute to the

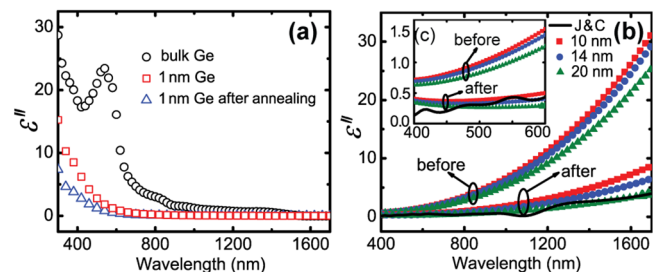


FIG. 1. (Color online) (a) Retrieved imaginary part of permittivity (ϵ'') of Ge. (b) Retrieved ϵ'' of SFs with different thicknesses on 1 nm Ge wetting layers before and after annealing. (c) Retrieved ϵ'' of SFs before and after annealing in the 400–600 nm wavelength range.

^{a)}Electronic mail: shalaev@purdue.edu.

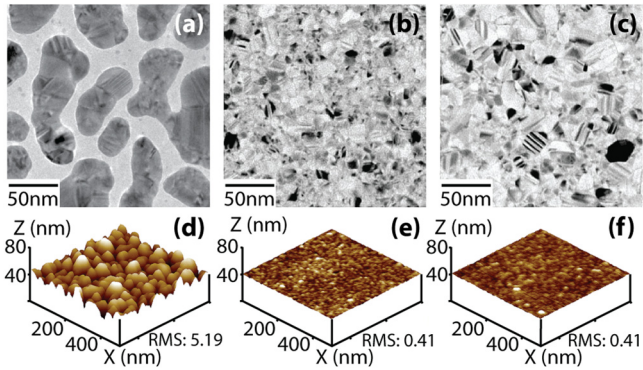


FIG. 2. (Color online) TEM images of 10 nm SFs (a) without Ge, (b) with 1 nm Ge, and (c) with 1 nm Ge and after annealing at 320 °C for 3 min. AFM topographs of 10 nm SFs (d) without Ge, (e) with 1 nm Ge, and (f) with 1 nm Ge and after annealing at 320 °C for 3 min.

loss at wavelengths shorter than 400 nm, hence the contribution from the Lorentz terms is negligible in the wavelength range of 400–1700 nm.

The loss (ϵ'') values retrieved from the measured spectra of SFs with thicknesses ranging from 10 to 20 nm have been compared with the commonly accepted Johnson and Christy's results for bulk Ag,¹ as shown in Figs. 1(b) and 1(c). The ultrathin, continuous SFs show a size effect as evidenced by an increased ϵ'' compared to that of bulk silver. This size effect loss can be explained by a shortened mean-free-path.^{2,12} For an ultrathin (<30 nm) SF, the grain sizes are extremely small. When the size of the metal structures, such as nanoparticles and grains, becomes smaller than the electron mean free path in the bulk material, which is about 52 nm,¹³ the electrons experience collisions with the grain boundaries. This results in an increase in the collision rate, which in turn increases the damping rate. The damping rate γ_p therefore depends on the grain sizes in the film. Hence, an additional size-dependent term should be included in the damping rate as follows:^{2,12}

$$\gamma_p = \gamma_\infty + Av_F/R, \quad (2)$$

where $\gamma_\infty = 0.021$ eV is assumed constant for bulk Ag, $v_F = 1.39 \times 10^6$ m/s ($\hbar v_F = 0.915$ eV nm) is the Fermi velocity,¹⁴ R is the metal particle radius or grain size, and the A parameter is a constant around one that depends on the details of the scattering process and the type of material surrounding the particle or grain.

In order to reduce the optical losses, an annealing treatment was explored for our samples. Such a thermal annealing treatment can reduce the loss by allowing grains in the polycrystalline SFs to grow in size, thereby reducing the size-dependent term in the damping rate that arises from electron scattering at grain boundaries. A group of 10 nm SFs with and without a Ge wetting layer were fabricated on glass substrates for x-ray diffraction (XRD, PANalytical X'Pert) measurements and also on special 30-nm-thick SiN membranes for transmission electron microscopy (TEM, Tecnai) measurements. In our XRD experiments, the grain sizes in the SFs are determined from the (111) reflections using the standard Debye–Scherrer formulation.¹⁵ The XRD measurements of the 10 nm Ag/1 nm Ge/10 nm SiO₂/glass samples show that the average vertical grain sizes (D_\perp) both before and after annealing are almost constant at about 7.7 nm. Figure 2(a) shows a TEM image of 10 nm SF directly deposited

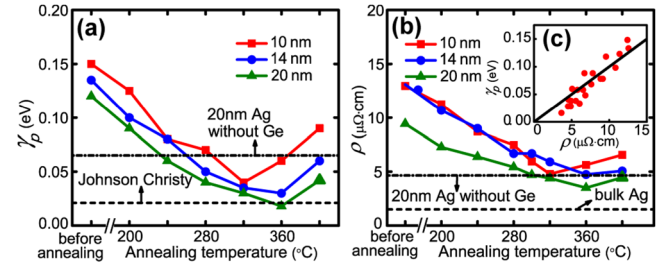


FIG. 3. (Color online) (a) Experimentally retrieved damping rate (γ_p) curves and (b) Measured resistivity (ρ) of SFs at different thicknesses on a 1 nm Ge layer after annealing at different temperatures for 3 minutes. (c) Linear relation between the γ_p and ρ in the SFs.

on a 10 nm SiO₂/30 nm SiN substrate. Clearly, the SF is not yet continuous. In contrast, the image in Fig. 2(b) shows that a 10 nm SF deposited on a 1 nm Ge/10 nm SiO₂/30 nm SiN substrate is already continuous. In addition, our TEM results indicate that the lateral extension (D_\parallel) of the grains in the film of Fig. 2(b) are around 5–10 nm, which is close to the vertical grain sizes (D_\perp). Figure 2(c) shows that the grains have grown much larger laterally after an annealing treatment of 320 °C for 3 min. Although the SF thickness is only 10 nm, the lateral extension (D_\parallel) of the grains after annealing reaches 25–40 nm. These lateral grain sizes are much larger than the vertical grain sizes, which are limited by the 10 nm film thickness. The measured TEM and XRD results indicate that the Ge sublayer facilitates the Ag grain growth in preferred orientations in the lateral directions during the annealing process, a process known as texturing.

The surface morphologies of the Ag samples were observed at room temperature using an atomic force microscope (AFM, Veeco Dimension 3100) in tapping mode with a scan size of $0.5 \mu\text{m} \times 0.5 \mu\text{m}$, a scan rate of 1 Hz and standard Si tapping-mode tips. The collected AFM topographies were characterized by computing the root-mean-square (rms) surface roughness values of each sample. Typical AFM topographies from 10 nm SFs are shown in Figs. 2(d)–2(f). The rms roughness of 10 nm SFs deposited on Ge/SiO₂/glass substrates both before and after proper annealing treatments are only about 0.4 nm, while the rms roughness of a 10 nm SF directly deposited on SiO₂/glass substrate is as high as 5.189 nm. This result confirms the previously published results^{7,8} that the addition of a Ge layer can significantly reduce the surface roughness of SFs. In addition, our roughness measurements show that a proper thermal annealing treatment did not increase the surface roughness of an SF deposited on a Ge layer.

The effects of our annealing treatment are quite sensitive to conditions such as the temperature and time. The treatment is “rapid” because a 3–5 min duration provides the best annealing effect for the majority of our ultrathin SFs. Longer annealing times do not further reduce the loss in the SFs but rather result in increased loss due to rougher surfaces and even cracks in the films. Another important factor in the annealing process is the temperature. Figure 3(a) shows the retrieved damping rate of SFs with varied thicknesses (10, 14, and 20 nm) deposited on a 1 nm Ge layer after 3 min annealing at different temperatures. Within the proper annealing temperature range (200–400 °C), a relatively high annealing temperature will provide better loss-reducing effects, and at the same time the SFs still maintain a smooth

surface as shown in Fig. 2(c). When the annealing temperature is increased beyond a critical point T_C , the SFs will be over-annealed and the grains in the films grow vertically, causing the SFs to become rougher or even semicontinuous. The over-annealed SFs show much higher loss due to the rough surface and additional defects in the films. Our AFM analysis shows that the rms roughness of an over-annealed 10 nm SF (420 °C, 3 min) is 3.81 nm, which is much larger than the original value (0.4 nm). Therefore, the annealing conditions must be carefully controlled so that the lowest loss for the SFs can be achieved. The experimental results in Figs. 1(b), 1(c), and 3 show that a thermal annealing treatment can reduce the losses in the ultrathin SFs by a factor of 3.3–6.6 and bring the loss close to that of the bulk Ag value without degrading the overall film roughness.

The annealing treatment is not effective for SFs without a Ge wetting layer because the treatment allows the grains to grow both laterally and vertically in such films. The maximum grain sizes for a continuous SF deposited on a dielectric (SiO_2) substrate are restricted by the film thickness itself. Even a low-temperature annealing (80–160 °C) for a 20 nm SF without a Ge layer will result in an overgrowth of the grains, leading to a rough surface and even cracks or voids in the film. Hence annealing treatments usually increase the surface roughness and increase the loss in SFs without a Ge layer. However, due to the Ge wetting effect the Ag grain growth in the lateral directions is preferred and growth in the vertical direction is limited during the annealing process. A proper annealing treatment for SFs on Ge layers allows the grains to grow but does not increase the surface roughness.

Our experiments also show that the annealing treatment is effective for silver-silica multilayer composite films, which are the basic structures of recent superlens and hyperlens designs. For these experiments, a group of (10 nm Ag/1 nm Ge/10 nm SiO_2)₃/glass samples were prepared as mentioned above. The measured rms roughnesses of these composite films were about 0.4 nm, which is close to that of a single-layer SF on a Ge layer. The damping rate of the 10 nm Ag sublayers were reduced from 0.15 to 0.040 eV after annealing for 10 min at 400 °C. Note that these silver-silica multilayer films required somewhat higher temperatures and longer times for proper annealing due to their larger total thicknesses.

The annealing effects were also studied by measuring the sheet resistances (R_S) of the SFs through a four-point probe method using a Jandel Multi Height probe with a RM3-AR test unit. The resistivities were then calculated by $\rho = R_S d$, where the d is the film thickness. The results of these measurements are shown in Fig. 3(b). According to the Fuch–Sondheimer–Mayadas scattering theory,¹⁶ the resistivity of an Ag thin film can be expressed as $\rho = \rho_0 + \rho_{SS} + \rho_{GB} + \rho_{SR}$. In addition to the bulk resistivity value ρ_0 , the total resistivity also includes contributions from surface scattering $\rho_{SS} = \rho_0 C/d$, grain-boundary scattering $\rho_{GB} = \rho_0 K/D$, and roughness $\rho_{SR} = \rho_0 C B^2/d^3$. Here D is the mean grain size, while K , C , and B are scattering constants. The annealing treatment can significantly reduce the ρ_{GB} term by enlarging the lateral extensions of the grains, while the smoothing ef-

fect from the Ge layer can reduce the ρ_{SR} term for ultrathin SFs. Due to the smoother surface and larger lateral extensions of the grains in the film, the measured ρ value of a 20-nm SF deposited on a 1-nm Ge layer after annealing at 360 °C for 3 minutes is lower than that of a 20-nm SF directly deposited on a SiO_2 /glass substrate. Figure 3(c) shows that the resistivity (ρ) of the SF is linearly proportional to the damping rate (γ_p) in the film following the formula $\gamma_p = \epsilon_0 \omega_p^2 \rho$, where ϵ_0 is the dielectric constant of vacuum and ω_p is the plasma frequency.¹⁶ Hence, the reduced ρ value of the ultrathin SFs is further evidence of reduced loss in the films.

In summary, we have demonstrated that a thermal annealing treatment under optimized conditions can reduce the optical losses in ultrathin SFs deposited on a Ge wetting layer to values as low as the bulk material value and at the same time maintain an ultrasmooth surface. This effect is sensitive to the annealing temperature and time, both of which should be carefully controlled. Moreover, our experimental results show that this annealing treatment is also effective for Ag– SiO_2 multilayer composite films, although these films require relatively higher annealing temperatures and longer times. We therefore conclude that ultrathin, ultrasmooth, and low-loss SFs and Ag– SiO_2 multilayer composite films can be achieved using a Ge wetting layer and a thermal annealing treatment. These results should be of interest to researchers in the areas of plasmonics and metamaterials, where low loss in thin SFs is an important area of interest.

This work was partially supported by the ARO-MURI Grant Nos. 50342-PH-MUR and W911NF-09-1-0539 and by the NSF-PREM Grant No. DMR 0611430.

¹P. B. Johnson and R. W. Christy, *Phys. Rev. B* **6**, 4370 (1972).

²V. P. Drachev, U. K. Chettiar, A. V. Kildishev, H. K. Yuan, W. S. Cai, and V. M. Shalaev, *Opt. Express* **16**, 1186 (2008).

³G. Dolling, M. Wegener, C. M. Soukoulis, and S. Linden, *Opt. Lett.* **32**, 53 (2007).

⁴S. Xiao, U. K. Chettiar, A. V. Kildishev, V. P. Drachev, and V. M. Shalaev, *Opt. Lett.* **34**, 3478 (2009).

⁵N. Fang, H. Lee, C. Sun, and X. Zhang, *Science* **308**, 534 (2005).

⁶Z. Jacob, L. V. Alekseyev, and E. Narimanov, *J. Opt. Soc. Am. A Opt. Image Sci. Vis.* **24**, A52 (2007).

⁷W. Chen, M. D. Thoreson, S. Ishii, A. V. Kildishev, and V. M. Shalaev, *Opt. Express* **18**, 5124 (2010).

⁸V. Logeeswaran, N. P. Kobayashi, M. S. Islam, W. Wu, P. Chaturvedi, N. X. Fang, S. Y. Wang, and R. S. Williams, *Nano Lett.* **9**, 178 (2009).

⁹P. Yeh, *Optical Waves in Layered Media*, 2nd ed. (Wiley, New York, 2005).

¹⁰S. Ishii, U. K. Chettiar, X. Ni, and A. V. Kildishev (2008), "PhotonicsRT: Wave Propagation in Multilayer Structures," DOI:10254/nanohubr5968.8.

¹¹X. Ni, Z. Liu, and A. V. Kildishev (2007), "PhotonicsDB: Optical Constants," DOI:10254/nanohubr3692.5.

¹²A. Pinchuk, U. Kreibitz, and A. Hilger, *Surf. Sci.* **557**, 269 (2004).

¹³U. K. Eibig and C. V. Fragstein, *Z. Phys. A: Hadrons Nucl.* **224**, 307 (1969).

¹⁴N. P. Singh, S. C. Gupta, and B. R. Sood, *Am. J. Phys.* **70**, 845 (2002).

¹⁵G. Chen, P. Hui, K. Pita, P. Hing, and L. Kong, *Appl. Phys. A: Mater. Sci. Process.* **80**, 659 (2005).

¹⁶P. Wissmann and H.-U. Finzel, *Electrical Resistivity of Thin Metal Films* (Springer, Berlin, New York, 2007).